

## 엔드밀링에서 순간전단면을 이용한 절삭력 모델 연구

홍민성\*

(논문접수일 2002. 3. 12, 심사완료일 2002. 6. 8)

### A Study on the Instantaneous Shear Plane Based Cutting Force Model for End Milling

Min-Sung Hong\*

#### Abstract

The purpose of this paper is to further extend the theoretical understanding of the dynamic end milling process and to derive a computational model to predict the milling force components. A comparative assessment of different cutting force models is performed to demonstrate that the instantaneous shear plane based formulation is physically sound and offers the best agreement with experimental results. The procedure for the calculation of the model parameters used in the cutting force model, based on experimental data, has been presented. The validity of the proposed computational model has been experimentally verified through a series of cutting tests.

**Key Words** : Instantaneous Shear Plane, Cutting Force, End Milling

### 1. Introduction

Accurate modeling of the cutting forces is necessary for the prediction of machining performance and to determine the mechanisms and machining parameters that affect the stability of machining operations. Modeling of milling operations has been an important research issue for a long time. While early investigations focused on the estimation of average cutting forces and power, the current interests are mainly in the

area of process stability, part geometry, surface texture, and cutting condition monitoring.

The cutting forces in machining operations are often found from empirical equations. The required constants or parameters for these equations are determined experimentally. These techniques are useful and necessary, however, the resulting equations and parameters are often restricted to a particular operation and the conditions tested.

A disadvantage apparent from the overview of recent

\* 주저자, 아주대학교 기계 및 산업공학부 (mshong0922@empal.com)  
주소: 442-749 경기도 수원시 팔달구 원천동 산 5번지, Tel: 031-219-2526

metal removal research is the lack of a compelling physical reason for modeling and predicting cutting forces as being proportional to the undeformed chip cross section area or the combination of the instantaneous depth of cut and penetration rate in particular under dynamic cutting conditions. As it is well established by examination of photomicrographs of a partially formed chip the material is deformed by a shearing process along the shear zone/plane.<sup>(1)</sup> The material deformation rate is very high along the shear plane as a consequence of a very thin region in which shear occurs. In this sense, the cutting force components should have been associated with the area of the shear plane. However, the shear plane area is difficult to calculate since its direction is affected by the instantaneous cutting velocity, which is also a function of time, and also by the machined surface cut in a previous tool pass. Therefore, the concept that the chips are sheared from the workpiece is well perceived but seldom used in machining performance prediction.

Because of the complexity of calculations many researchers have used the undeformed chip thickness model to predict cutting forces. This is basically due to the difficulty of measuring the length of the shear line and to represent it as a function of measurable variables such as the undeformed chip thickness, vibration velocity, and accelerations. As a consequence, the linear force model that proportionally relates the undeformed chip thickness to the cutting force is widely used in analysis and simulation models.

To achieve a more accurate prediction of dynamic force components, the physically more adequate and meaningful approach to the evaluation and simulation of the dynamic cutting processes will be adopted. Therefore, in this paper a cutting force model for end milling operations based on the instantaneous shear plane will be derived and experimentally verified.

## 2. Cutting Force Models in Milling

Many past efforts have concentrated on the analysis of general three-dimensional cutting mechanics for oblique

cutting. Shaw et al.<sup>(2)</sup> analyzed oblique cutting and introduced the effective rake and effective shear angles by treating the material flow in three-dimensional cutting as modification of the plane strain model of orthogonal cutting. Usui et al.<sup>(3)</sup> further developed the three-dimensional cutting force model for a single-point tool in which the process is interpreted as a piling up of orthogonal cuts along the cutting edge.

It is generally assumed that the shear plane keeps a constant direction in space though it is well known that the shear plane is varying in a way not yet fully understood. In early studies, Merchant<sup>(4)</sup> and Lee and Shafer<sup>(5)</sup> have proposed a shear angle  $\phi$  expression as a function of the difference between the mean angle of friction on the tool face  $\beta$  and the rake angle  $\gamma$ :

$$\phi = c_1 + c_2(\beta - \gamma) \quad (1)$$

where  $c_1$  and  $c_2$  are constant coefficients. This expression is based on the assumption that the shear angle depends on the mean angle of friction on the tool surface.

An approximation of the shear angle including the undeformed chip thickness effect is<sup>(6)</sup>:

$$\phi = \frac{\pi}{4} + \frac{\gamma - \beta}{2} + \frac{1}{2} \tan^{-1} \left\{ a \cdot w \cdot \cos \frac{\omega}{v} [t + t_h(t)] \right\} \quad (2)$$

where  $a$  is the amplitude of variation of the undeformed chip thickness,  $v$  is the cutting velocity,  $\omega$  is the angular velocity of the tool or the workpiece,  $t$  is the period of the cutting wave, and  $t_h(t)$  is time required for the tool to travel the distance equal to the projection of the shear plane length on the cutting direction.

The work of Usui et al.<sup>(3)</sup> for oblique single point cutting that utilizes a nominal shear plane area based force model, which shows very close agreement to the experimental results, would suggest that a shear plane based approach is plausible. Therefore, in the present work a cutting force model for end milling processes based on the instantaneous shear plane will be formulated and derived.

## 2.1 Comparison of Different Force Models

There are numerous algorithms for estimating cutting forces by considering cutting forces as a function of the:

- (A) instantaneous shear plane area,
- (B) nominal undeformed chip cross section area,
- (C) instantaneous undeformed chip cross section area,
- (D) nominal undeformed chip cross section area and a penetration rate term.

In order to assess the quantitative and qualitative differences between the four models a numerical approach was adopted. For this purpose, a computer program was written to calculate the non-dimensional cutting force,  $f_c(t)$ , and thrust force,  $f_t(t)$ , for the orthogonal cutting process which are defined as:

$$f_c(t) = \frac{F_c(t)}{-bc\tau} \quad (3a)$$

$$f_t(t) = \frac{F_t(t)}{-bc\tau} \quad (3b)$$

where  $F_c(t)$  and  $F_t(t)$  are the cutting and thrust forces,  $b$  and  $c$  are the width of cut and the mean undeformed chip thickness, and  $\tau$  is the average shear stress on the shear plane, respectively.

For the shear plane based model (designated as model A)  $F_c(t)$  and  $F_t(t)$  can be represented as<sup>(4)</sup>:

$$F_c(t) = \frac{bl(t)\tau \cos(\beta - \gamma)}{\cos(\phi + \beta - \gamma)} \quad (4a)$$

$$F_t(t) = \frac{bl(t)\tau \sin(\beta - \gamma)}{\cos(\phi + \beta - \gamma)} \quad (4b)$$

where the instantaneous shear line length  $l(t)$  is the length measured from the cutting edge to the free surface along the direction which is tilted at an angle  $\phi$  to the nominal cutting velocity  $\vec{V}_n(t)$ .

The undeformed chip cross-section area model, which is widely used in modeling metal cutting operations, can be expressed as (model B)<sup>(7)</sup>:

$$F_c(t) = -k_c A = -bk_c g(t) \quad (5a)$$

$$F_t(t) = -k_d A = -bk_d g(t) \quad (5b)$$

where the nominal undeformed chip thickness  $g(t)$  is perpendicular to  $\vec{V}_n(t)$ ,  $k_c$  is the cutting stiffness given by  $k_c = \tau / \sin \phi$ , and  $k_d$  is a parameter which depends on the workpiece material for mild steel  $k_d = 0.3 \cdot k_c$ .

For the instantaneous undeformed chip cross section area based model, which is the extension of the instantaneous undeformed chip thickness model, can be expressed as (model C):

$$F_c(t) = -k_c A_c = -bk_c h(t) \quad (6a)$$

$$F_t(t) = -k_d A_c = -bk_d h(t) \quad (6b)$$

where the instantaneous undeformed chip thickness  $h(t)$  is perpendicular to the instantaneous velocity vector  $\vec{V}(t)$ . For comparison purposes the values for  $k_c$  and  $k_d$  used in Eqs. 5 and 6 will be assumed the same. The principal physical shortcoming of the last two models is the fact that they do not consider the phase shift between consecutive waves in dynamic cutting.

To rectify this shortcoming of the above two models and to bring the model predictions closer to physical reality and agreement with experimental results a penetration rate term  $\dot{g}(t)$  is generally added to the model given by Eq. 5 to yield (model D)<sup>(8,9)</sup>:

$$F_c(t) = -bk_c g(t) - bb_c \dot{g}(t) \quad (7a)$$

$$F_t(t) = -bk_d g(t) - bb_d \dot{g}(t) \quad (7b)$$

where  $b_c$  and  $b_d$  represent the damping in the cutting and thrust directions, respectively. The penetration rate, which is in the form of the first derivative of the undeformed chip thickness, in essence introduces a phase shift between the dynamic force oscillation and the tool vibration.

The comparison between these models will be discussed with respect to different physical parameters to show the characteristics of different models in the following sub-sections.

**Influence of Phase Shift**

Figure 1 shows the non-dimensional cutting and thrust forces,  $f_c(t)$  and  $f_t(t)$ , versus the non-dimensional length,  $x/\lambda$ , for the four models, where  $x$  is the coordinate of the cutting edge and where  $y_1 = a \cdot \sin(2\pi x/\lambda)$  and  $y_2 = c + a \cdot \sin(2\pi x/\lambda + \Psi)$  are used to model the cutting waves, i.e., the inner and outer modulations respectively. In these simulations  $c=1$ ,  $k_d/k_c=0.3$ , and the simulation range for  $x$  is 0 to  $2\pi$ . The shear plane model is nonlinear when  $\vec{V}(t) \neq \text{constant}$  because of the phase shift term implicitly contained in the shear line length. Model A is generally in phase with models C and D but not with model B which means that models C and D also contain the nonlinear phase shift term because the magnitude and the direction of the force defined by model C is affected by  $\vec{V}(t)$  and the penetration rate term in model D implicitly contains the nonlinear phase shift term. The shapes of the cutting and thrust forces are affected by the phase shift between  $y_1$  and  $y_2$  as evidenced by Fig. 1. The variations of the force components are larger with larger phase shift.

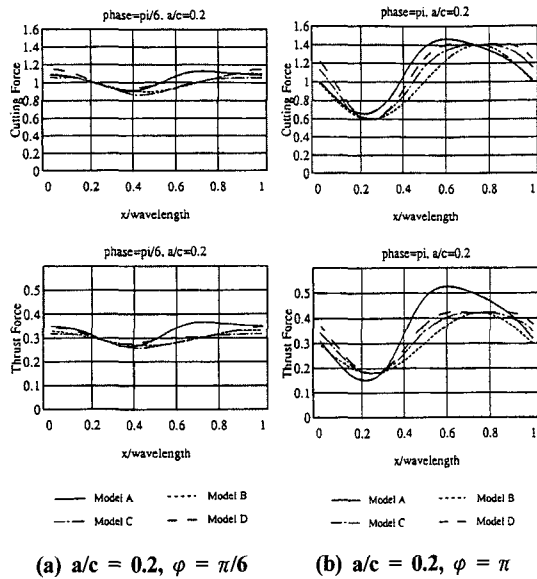


Fig. 1 Comparison of different cutting force models

**Influence of Vibration Amplitude**

Considering conditions with larger vibration amplitudes, shown in Fig. 2, the shapes of the cutting and thrust force components for model A have significantly changed. The differences between model A and the other three models becomes more pronounced for larger vibration amplitudes when compared with Fig. 2. When cutting is performed in the region from  $x=0.15\lambda$  to  $x=0.35\lambda$  for  $\Psi = \pi$ , where the workpiece material has been removed by a previous cut, the non-dimensional force components become equal to zero, i.e.,  $f_t(t) = f_c(t) = 0$ .

**Influence of Cutting Velocity**

The forces calculated by using models B, C, and D become identical when the cutting velocity  $\vec{V}(t) = \text{constant}$  ( $\gamma_f=0$ ) which corresponds to the case of wave removal (outer modulation). However, the shear plane model (model A) still exhibits a nonlinear property with respect to the undeformed chip thickness that distinguishes it from the other three models. Therefore, the use of models B and D for cutting force calculations might lead to poor results for certain cutting conditions and

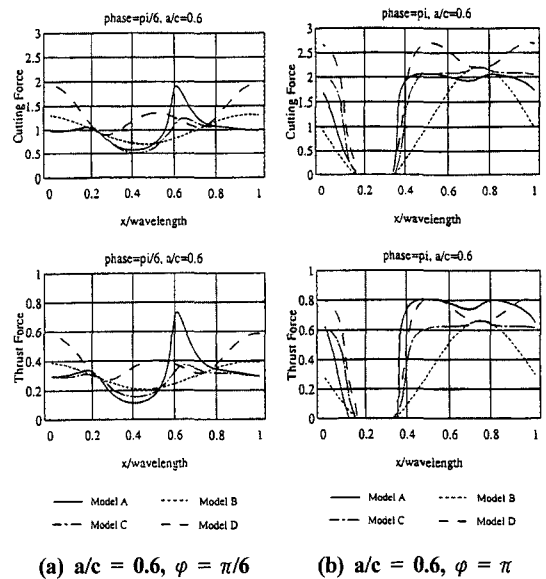


Fig. 2 Comparison of different cutting force models

may prevent a clear physical insight into the mechanisms of the material removal process.

#### *Influence of Vibration Frequency*

When machining in the presence of high frequency, low amplitude vibrations the penetration rate term in Eq. 7 (model D) will become the dominant term in calculating the cutting forces and the calculated forces will show large deviations from experimental results. This anomaly of model D corresponds to wave removal with  $y_1=0$  and  $y_2=c+a \cdot \sin(20\pi x/\lambda)$  in which a vibration frequency ten times higher than that in Fig. 1 is used. The forces calculated by using model D are much larger than the force components calculated by the other cutting force models.

Based on the aforementioned comparisons and discussions the obvious differences between the non-dimensional forces generated by different cutting force models were indicated. The penetration rate model (model D) yields unreasonable results for high frequency wave removal machining. The nominal cutting area based model (model B) cannot adequately reflect the phase shifts effect due to its proportional nature. The results generated by the instantaneous undeformed chip cross section area model (model C) are close to the shear plane model for certain conditions because they are related to the instantaneous cutting velocity. The shear plane based cutting force model is physically more reasonable and in better agreement with observations.<sup>(1,3,10)</sup> Finally, the computational load for model C is approximately equal to that of model A. There is virtually no experimental evidence in support of concept C in previous research.

Therefore, to improve the analysis of milling operations one major goal of this research is to derive a shear plane based cutting force model and the associated algorithms to effectively calculate the instantaneous shear plane area to predict the cutting forces.

### **3. Shear Plane Based Cutting Force Model for end Milling Operations**

The starting point of the analysis will rest on the usual discretization of the cutter's edges into elemental cutting edge segments.<sup>(11,12)</sup> Each elemental cutting edge will be considered as an oblique cutting tool, therefore, the two dimensional orthogonal cutting force model can not be applied to model milling operations. Therefore, a three dimensional cutting force model will be developed by using oblique cutting test data.

#### **3.1 Model Formulation**

The instantaneous shear plane area will be taken as a measure of the force applied by the cutting tool. The cutting force model to be discussed next is derived based upon these assumptions:

- (1) The primary deformation occurs in a very thin zone adjacent to the shear plane.
- (2) A continuous or segmented chip is formed with no built-up edge.
- (3) The minor effects of secondary shear along the tool chip interface will be ignored.
- (4) The contact force between the tool and the workpiece will be considered constant throughout the modeling of cutting forces.
- (5) The stresses along the tool face and shear plane are uniformly distributed.
- (6) The cutting force of the cutter's end can be neglected during the calculation of the three dimensional forces because the magnitude of this force is only a small fraction of the cutting force exerted by the periphery of the cutter under practical cutting conditions.

#### *The Resultant Force on the Elemental Cutting Edges*

The end-milling operation is an oblique cutting process because of the helix angle that causes the cutting edge to be inclined with respect to the cutting velocity. Another characteristic of the process is that the undeformed chip thickness and the instantaneous shear line length are continuously changing.

The resultant force on the elemental cutting edge is the vector sum of force components. After neglecting the end force components the resultant force can be represented as:

$$\begin{aligned} \vec{R}_{i,j}(t) &= \vec{F}_{ci,j}(t) + \vec{F}_{ti,j}(t) + \vec{F}_{li,j}(t) \\ &= \vec{F}_{xi,j}(t) + \vec{F}_{yi,j}(t) + \vec{F}_{zi,j}(t) \end{aligned} \quad (8)$$

where  $\vec{F}_{ci,j}(t)$ ,  $\vec{F}_{ti,j}(t)$ , and  $\vec{F}_{li,j}(t)$  are the cutting, thrust, and lateral forces exerted on the periphery of the cutter.

On the other hand, the resultant cutting force is the sum of the force to shear the work material into chips and of the contact force:

$$\vec{R}_{i,j}(t) = \vec{R}_{2i,j}(t) + \vec{F}_{ii,j}(t) \quad (9)$$

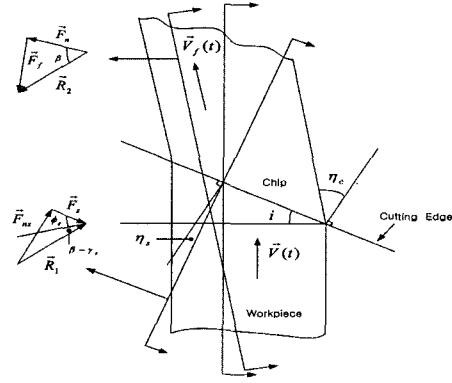
where  $\vec{R}_{2i,j}(t)$  is the resultant cutting force exerted by the elemental cutting edge to remove the chip and  $\vec{F}_{ii,j}(t)$  is the corresponding contact force between the elemental cutting edge and the workpiece. Considering the chip as a free body,  $\vec{R}_{2i,j}(t)$  can be represented by the friction force  $\vec{F}_{fi,j}(t)$  and the normal force on the tool face  $\vec{F}_{ni,j}(t)$ . From Fig. 3 we have:

$$\vec{F}_{ni,j}(t) = \vec{R}_{2i,j}(t) \cos \beta(t) \quad (10a)$$

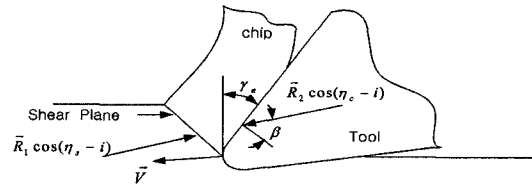
$$\vec{F}_{fi,j}(t) = \vec{R}_{2i,j}(t) \sin \beta(t) \quad (10b)$$

where  $\beta(t)$  is the instantaneous friction angle on the tool surface. In turn, the resultant force on the shear plane  $\vec{R}_{1i,j}(t)$  can be represented by the shear force  $\vec{F}_{si,j}(t)$  and the normal force  $\vec{F}_{nsi,j}(t)$  on the shear plane. Since  $\vec{R}_{1i,j}(t)$  and  $\vec{R}_{2i,j}(t)$  are not collinear, the difference between them is related to the change in the momentum of the material crossing the shear plane.

The components of the two resultant forces are balanced on the plane that is normal to the plane that contains the cutting edge and the cutting velocity as shown in Fig. 3, that is



(a) Plan view of oblique cutting



(b) Side view of oblique cutting

Fig. 3 Force balance on the chip surface

$$R_{1i,j}(t) \cos(\eta_s(t) - i) = R_{2i,j}(t) \cos(\eta_c - i) \quad (11)$$

The shear force needed to shear the chip can be represented as the product of the shear stress,  $\tau$ , and of the elemental shear plane area,  $A_{si,j}(t)$ . By assuming that the shear stress is constant and uniformly distributed on the shear plane<sup>(1)</sup>:

$$\vec{F}_{si,j}(t) = \tau A_{si,j}(t) \quad (12)$$

From the experimental results of Usui et al.<sup>(3)</sup>  $\tau$  can be assumed constant in calculating the shear force.

### The Resultant Cutting Force Model

Separating the resultant cutting force in Eq. 9 into the cutting and thrust components, which are parallel and perpendicular to the instantaneous cutting velocity, and the lateral force component perpendicular to the plane formed by  $\vec{F}_{ci,j}(t)$  and  $\vec{F}_{ti,j}(t)$ , we have

$$F_{ci,j}(t) = F_{ni,j}(t) \cos \gamma_n \cos i + F_{fi,j}(t) \sin \gamma_n + F_{if,i,j} \quad (12a)$$

$$F_{fi,j}(t) = -F_{ni,j}(t) \sin \gamma_n + F_{fi,j} \cos \gamma_n \cos \eta_c + F_{ini,j} \quad (12b)$$

$$F_{if,i,j}(t) = -F_{ni,j}(t) \cos \gamma_n + \sin i - F_{fi,j}(t) \cos \gamma_n \cos \eta_c \quad (12c)$$

### 3.2 Determination of Parameters Used in the Cutting Force Model

The use of Eq. 12 to calculate the cutting force components requires the knowledge of the parameters  $\tau$ ,  $\beta$ ,  $V(t)$ ,  $\phi_e$ , and  $\gamma_e$  and of the contact force coefficients. A method to calculate the aforementioned parameters from measurements of cutter geometry and cutting test data for different workpiece materials will be discussed in Appendix. It will be assumed that the values of  $\tau$ ,  $\beta$ ,  $\phi_e$ , and  $\gamma_e$  remain constant during the process.

## 4. Verification of the Force Model

A number of cutting tests have been conducted to verify the feasibility of the proposed method and of the derived force model. Cutting force components were measured by a three-component dynamometer (Kistler type 9255B). The accelerations in the X, Y, and Z directions were measured by accelerometers (PCB type U353, UJ353, and 302A02) mounted on a specially machined aluminum cube attached to the spindle housing of the machining center. The workpiece was 6061 Aluminum.

The chip thickness was measured by using a Mitutoyo micrometer M820-25V with a ball tips on both ends. Two one-tooth cutters were used. One of them had a 38.1 mm (1.5 in.) diameter with a carbide insert with zero helix angle and flat cutting edge (zero rake angle) so that the milling operation with this cutter can be considered as an orthogonal cut. The other one was a 19.05 mm (0.75 in.) cutter made of High Speed Steel (HSS) with a 40° helix angle and  $\gamma_n = 15^\circ$ . Three materials were used as the workpiece: AISI-1018 hot-

**Table 1 Cutting force coefficients**

	$k_{lc}$ (KM/m)	$k_{rt}$ (KM/m)	$k_{2c}$ (KM/m <sup>2</sup> )	$k_{2t}$ (KM/m <sup>2</sup> )
Al	2.2	2.85	304.11	317.33
Brass	1.78	2.12	209.23	100.69
Steel	1.45	2.11	420.42	246.18

**Table 2 Measured chip thickness and calculated cutting parameters**

	Steel	Brass	Al
$t_c$ (mm)	0.146	0.057	0.113
$\phi_n$ (deg.)	19.95	47.63	25.77
$\gamma_e$ (deg.)	34.41	34.41	34.41
$\eta_s$ (deg.)	29.64	5.13	25.44
$\phi_e$ (deg.)	19.31	55.13	25.96
$\beta$ (deg.)	49.63	44.98	65.50
$\tau$ (NM/m <sup>2</sup> )	108.82	64.28	85.80

rolled steel, free-machining alloy 360 brass, and 6061 Aluminum.

The cutting conditions were: feed = 3, 5, 15, 30, 45, and 60 mm/min, spindle speed = 100, 600, 1200 rpm, and width of cut = 0.5, 1, 2, 4, 6 mm, respectively. Table 1 shows the coefficients calculated from the measured cutting force data.

The measured chip thickness data and calculated parameters are listed in Table 2. The calculated friction angles for these material are consistent with the observations during the cutting tests that the chips for aluminum are continuous hence the ratio of friction force to the resultant force is higher and the friction angle is larger than that for steel and brass. The chips for the free-machining alloy 360 brass were sheared into needle-like pieces hence the contact area between chip and tool face is smaller and the shear angle is the largest among the three workpiece materials. The mean shear stresses on the shear plane were calculated by using the experimental data and Eq. A8 in Appendix for the three workpiece materials.

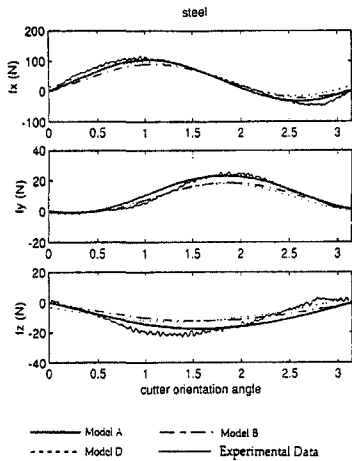


Fig. 4 Comparison of measured and predicted cutting forces steel

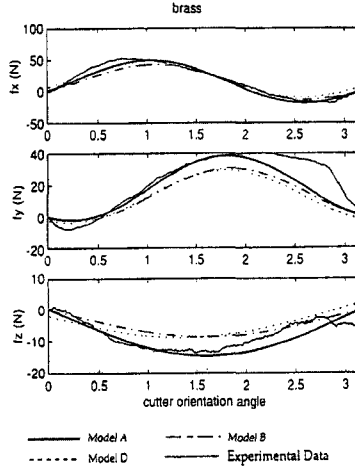


Fig. 5 Comparison of measured and predicted cutting forces brass

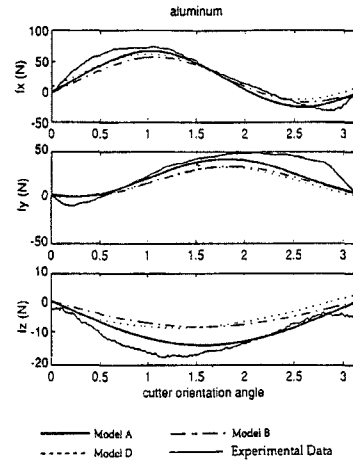


Fig. 6 Comparison of measured and predicted cutting forces aluminum

Figures 4 to 6, which correspond to oblique cutting with the  $40^\circ$  helix angle one tooth milling cutter, show the comparison between the measured and predicted cutting forces by using different force models. Model A is the shear plane based force model calculated by using Eqs. A6 and A7 in Appendix. Model B is the nominal undeformed chip thickness based force model calculated by using Eq. 5. Model D is the result of using the nominal undeformed chip thickness and penetration rate model given by Eq. 7. The forces based on models B and D were evaluated by using a simulation program with a similar architecture as the program for model A. The cutting conditions used were  $b=6\text{mm}$ ,  $w=600\text{rpm}$ , and  $f_t=0.05\text{ mm/tooth}$  with the one-tooth helical cutter. The results prove the good predictive capability of the

Table 3 The error percentages for average cutting forces for different models

	Force Models								
	A	B	D	A	B	D	A	B	D
	$F_x$			$F_y$			$F_z$		
Steel	3.54	6.32	6.01	2.66	3.85	3.9	5.20	8.89	8.72
Brass	2.96	5.16	5.09	4.11	9.94	9.88	8.65	20.11	19.97
Al	3.37	6.01	5.78	6.07	9.65	9.47	11.12	21.17	20.54

derived cutting force model especially with respect to the peak and average force predictions and the overall force shapes which are also in good agreement with the experimental data. They also show that the results of model A are closer to the experimental data than the results of models B and D. The errors in the average cutting forces calculated by using different models are listed in Table 3. It is evident that model A is consistently in better agreement with the measurements than the other models.

## 5. Conclusions

The following specific conclusions can be drawn:

- (1) A cutting force model based upon the instantaneous shear plane area was derived and compared to other cutting force models. The results show that the shear plane based force model is physically sound and better represents the machining process.
- (2) The proposed cutting force model was defined based on a discrete representation of the end milling process. The cutting edges of the milling cutter were divided into many segments, each considered as an oblique cutting edge. The resultant cutting forces were



computed as the sum of the elemental cutting forces composed of a chip shearing and of a tool-workpiece contact force component.

- (3) Algorithms for calculating the cutting process parameters used in the derived cutting force model were introduced.

## APPENDIX :

The general procedure to evaluate the cutting process parameters on the shear plane is the following:

- (1) Experimentally measure the cutting forces for different average undeformed chip thickness values. The average undeformed chip thickness is calculated as  $2f_i/\pi$ , where  $f_i$  is the feed per tooth.
- (2) Measure the cutter helix angle  $\eta$  and normal rake angle  $\gamma_n$ .
- (3) Calculate the normal shear angle  $\phi_n$  using Eq. A1 and the measured chip thickness ratio  $\gamma_t$ .

$$\phi_n(t) = \tan^{-1} \left[ \frac{r_t \cos \gamma_n(t)}{1 - r_t \sin \gamma_n(t)} \right] \quad (A1)$$

$$\eta_c = \cos^{-1} \left( \frac{b_c \cos i}{b} \right) \quad (A2)$$

$$\gamma_e(t) = \sin^{-1} \left[ \sin \gamma_n(t) \cos i \cos \eta_c + \sin \eta_c \sin i \right] \quad (A3)$$

- (4) The effective rake angle  $\gamma_e$  is obtained by Eqs. A2 and A3.
- (5) The shear flow angle  $\eta_s$  is obtained by using Eq. A4.

$$\eta_s(t) = \tan^{-1} \left[ \frac{\tan i \cos [\phi_n(t) - \gamma_n(t)] - \tan \eta_c \sin \phi_n(t)}{\cos \gamma_n(t)} \right] \quad (A4)$$

- (6) The effective shear angle  $\phi_e$  is calculated by using Eq. A5.

$$\phi_e(t) = \sin^{-1} \left[ \frac{\cos \gamma_e(t) \eta_s(t)}{\cos \eta_c \cos \gamma_n(t)} \sin \phi_n(t) \right] \quad (A5)$$

- (7) To obtain the coefficients  $k_{2c}$  and  $k_{2t}$  the cutting and thrust forces are plotted versus the average undeformed chip thickness.

$$F_c = \frac{\tau A \cos(\eta_s - i) (\cos \beta \cos \gamma_n \cos i + \sin \beta \sin \gamma_n)}{\cos(\phi_e + \beta - \gamma_e)} + bk_{1c} \quad (A6)$$

$$F_t = \frac{\tau A \cos(\eta_s - i) (-\cos \beta \sin \gamma_n + \sin \beta \cos \gamma_n \cos \eta_c)}{\cos(\phi_e + \beta - \gamma_e)} + bk_{1t}$$

$$F_t = \frac{\tau A \cos(\eta_s - i) (-\cos \beta \sin \gamma_n + \sin \beta \cos \gamma_n \cos \eta_c)}{\cos(\phi_e + \beta - \gamma_e)} + bk_{1t} \quad (A7)$$

- By curve-fitting the data  $k_{2c}$  and  $k_{2t}$  are obtained as the slope of the lines. The contact force coefficients  $k_{1c}$  and  $k_{1t}$  correspond to the value of the cutting and thrust forces for a value of the undeformed chip thickness  $t = 0$ .
- (8) The shear stress can be calculated by

$$\tau = \frac{(k_{2c} \cos \beta + k_{2t} \sin \beta) \cos(\phi_e + \beta - \gamma_e) \sin \phi_e}{\cot i \cos \gamma_n \cos(\eta_s - i)} \quad (A8)$$

where the friction angle  $\beta$  is given by

$$\beta = \tan^{-1} \left[ \frac{\cos \gamma_n \cos i + \frac{k_{2c}}{k_{2t}} \sin \gamma_n}{\frac{k_{2c}}{k_{2t}} \cos \gamma_n \cos i - \sin \gamma_n} \right] \quad (A9)$$

## Reference

- (1) Shaw, M. C., *Metal Cutting Principle*, Oxford Science Publication, 1991.
- (2) Shaw, M. C., Cook, N., H., and Smith, P. A., "The Mechanics of Three dimensional Cutting Operations," *Trans. ASME*, Vol. 74, pp. 1055~1064, 1952.
- (3) Usui, E., Hirota, A., and Masuko, M., "Analytical Prediction of Three Dimensional Cutting Process, Part 1 Basic Cutting Model and Energy Approach," *Trans. ASME*, Vol. 100, pp. 222~228, 1978.
- (4) Merchant, M. E., "Basic Mechanics of the Metal

- Cutting Process," Trans ASME, Vol. 66, pp. 168~175, 1944.
- (5) Lee, E. H. and Shafer, B. W., "The Theory of Plasticity Applied to a Problem of Machining," J. of Applied Mechanics, Vol. 18, No. 4, pp. 405, 1951.
- (6) Albrecht, P., "Dynamics of the Metal Cutting Process," Journal of Engineering for Industry, Vol. 87, pp. 429~441. 1965.
- (7) Tlusty, J. and Ismail, F., "Special Aspects of Chatter in Milling," Journal of Vibration, Acoustics, Stress, and Reliability in Design, Vol. 105, pp. 24~32, 1983.
- (8) Minis, I., Yanushevsky, R., and Tembo, A., "Analysis of Linear and Nonlinear Chatter in Milling," Annals of the CIRP. Vol. 39, pp. 459~462, 1990.
- (9) Tobias, S. A., *Machine Tool Vibration*, Wiley, N. Y., 1965.
- (10) Armarego, E. J. A., and Epp, C., J., "An Investigation of Zero Helix Peripheral Up-Milling," Int. J. Mach. Tool Des. Res., Vol. 10, pp. 273~291, 1970.
- (11) Hong, M. S. and Ehmann, K. F., "Generation of Engineered Surfaces by the Surface-Shaping System," Int. J. Mach. Tools Manufact., Vol. 35, pp. 1269~1290, 1995.
- (12) Hong, M. S., "A Numerical Simulation on Cutting Force and Surface Roughness of the Face Milling," J. Korean Society of Mach. Tool Engr., Vol. 4, No. 4, pp. 16~24, 1995.